



# Gas sensing applications using magnetized cold plasma multilayers

Zaky A. Zaky<sup>1</sup> · Hussein A. Amer<sup>1</sup> · Bhuvneshwer Suthar<sup>2</sup> · Arafa H. Aly<sup>1</sup>

Received: 5 October 2021 / Accepted: 12 February 2022 / Published online: 13 March 2022  
© The Author(s) 2022

## Abstract

In this paper, we theoretically propose a novel magnetic field-dependent sensor using omnidirectional magnetized cold plasma photonic crystal in one dimension for TE polarization. The structure consists of asymmetric two periodic arrays from magnetized cold plasma and sample cavity layer. Between the periodic arrays, a sample cavity is sandwiched between two quartz layers. The methodology of the proposed detector depends on the appearance of a sensitive defect mode. The results clear that the defect mode frequency depends significantly on the refractive index of the sample, and it is extremely sensitive to incident angle changes, applied magnetic field, the number density of electrons, and sample layer thickness. The optimized proposed sensor has high sensitivity of 15.14 GHz/RIU, quality-factor of 527.32, and figure of merit of 1066.20 RIU<sup>-1</sup>, where RIU means refractive index unit. So, the proposed sensor can aid in solving many challenges in chemical and environmental applications.

**Keywords** Photonic crystal · Magnetized cold plasma · Gas sensor

## 1 Introduction

Photonic crystal (PC) is an optical structure of alternative materials with high and low refractive indices (Yablonovitch 2001; Yablonovitch and Gmitter 1989; Zaky and Aly 2021a; John 1987; Ayyub et al. 2013; Kushwaha et al. 2018). The periodicity of the refractive index causes forbidden frequency or wavelength region for photons that make it not allowed to propagate through the structure (John and Florescu 2001; Zaky et al. 2020; Tammam et al. 2021; Auguie et al. 2014; Boopathi et al. 2018; Panda and Devi 2020). Such forbidden frequency region is known as photonic bandgap (PBG) (Bikbaev et al. 2017; Zaky et al. 2021a; Aghajamali 2016; Zaky and Aly 2021b; Armstrong and O'Dwyer 2015; Afsari and Sarraf 2020; Abd El-Ghany et al. 2020). PC is used to modulate the flow of photons (Zaky and Aly 2020; Buswell et al. 2008; Zaky et al. 2021b; Gao et al. 2018; Aghajamali et al. 2015). According to the periodicity of the material,

---

✉ Zaky A. Zaky  
zaky.a.zaky@science.bsu.edu.eg

<sup>1</sup> TH-PPM Group, Physics Department, Faculty of Science, Beni-Suef University, Beni Suef, Egypt

<sup>2</sup> Department of Physics, M.L.B. Government College, Nokha, Bikaner, Rajasthan 334803, India

PC can be studied as one-dimensional (1D-PC) (Aly et al. 2020, 2021a; Beheiry et al. 2010; Aly and Zaky 2019; Zhou et al. 2021; Zhang et al. 2012; Zaky et al. 2021c, d; Meradi et al. 2022), two-dimensional (2D-PC) (Akahane et al. 2003; Zegadi et al. 2019), and three-dimensional PC (3D-PC) (Tandaechanurat et al. 2011; Zakhidov et al. 1998). Introducing a defect layer into the PC breaks the regular periodic arrangement and gives rise to appearing a defect localized mode in the PBG region (Zaky et al. 2021e). The defect localized mode can be utilized in different applications by characterizing the size of the defect layer as well as the dielectric constant of the defect layer. PCs have been studied as many potential clinical, physical and chemical applications such as switches, optical filters, multiplexers, sensors, etc. (Zaky et al. 2021f; Pandey et al. 2017; Zaky and Aly 2021c).

Optical sensor is one of the most interesting applications of PC, which have advantages over conventional devices as an ultra-fast response, ultra-compact size, and high sensitivity. Many kinds of sensors are investigated by scientists such as temperature detectors (Zaky and Aly 2021b), pressure sensors (Rajasekar and Robinson 2019), biosensors (Aly et al. 2021b), chemical sensors (Kim et al. 2009), and gas sensors (Zaky et al. 2020; Hidalgo et al. 2010). Because some gases are toxic and hazardous for health and the environment like CO, SO<sub>2</sub>, CO<sub>2</sub>, and N<sub>2</sub>O, optical gas sensors are safe to be used. Gas sensors have different applications in industries, home safety, environment monitor, the medical and agricultural field, etc.

Magnetized cold plasma (MCP) can be used as PC material by researchers (Liu and Wu 2021; Shiri et al. 2019; Sakai et al. 2007; Naderi Dehnavi et al. 2017; Nobahar et al. 2018; Kamboj et al. 2021; Askari et al. 2015; Awasthi et al. 2017, 2018; Lyubchanskii et al. 2003; Inoue et al. 2006). Chang et al. (2016) investigated magnetic field tunable filter application of 1D-PC using magnetized plasma and air multilayered structure in microwave frequency (Chang et al. 2016). Kumar et al. (2019) studied transmission properties of 1D-PC with magnetized plasma layers and used them as a tunable multichannel filter (Kumar et al. 2018). Wang et al. (2020) presented a multichannel filter device using a magnetized plasma layer in terahertz frequency (Wang et al. 2020).

In the present study, we propose a 1D-PC multilayered structure with MCP for gas sensing application. The defect layer as well as one of the regular layers are taken as a gas sample to detect the gas with the respective wavelength of the resonant mode.

## 2 Materials and simulation method

The proposed structure is a multilayered design of (AB)<sup>N</sup>/CDC/(AB)<sup>N</sup>/SiO<sub>2</sub>. N is the number of the unit cells (N=4), as illustrated in Fig. 1. Layer A and C are considered as MCP and quartz, while layer B and defect layer D are considered as gas samples. The incident medium is considered as air whereas the substrate is SiO<sub>2</sub>. The thickness of layer A, layer B, layer C, and layer D are considered as d<sub>1</sub>, d<sub>2</sub>, d<sub>q</sub>, and d<sub>sample</sub>, respectively.

The transfer matrix method is used for computing the transmittance of the proposed 1D-PC multilayered structure. The continuity condition of the electric and magnetic fields is used to obtain the field values. The matrix form of relations is utilized to obtain the field values on either side of each layer. The transfer matrix for jth layer is given as (Panda et al. 2021):

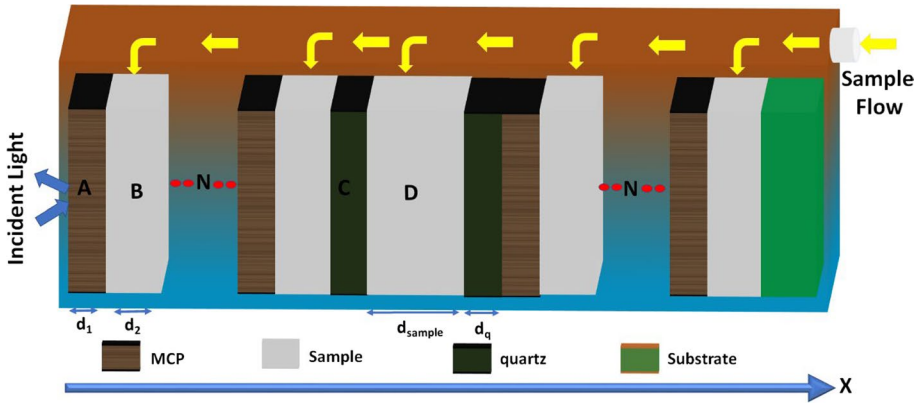


Fig. 1 Schematic illustration of proposed 1D-PC multilayered gas sensor

$$M_j = \begin{bmatrix} \cos \psi_j & -\frac{i}{q_j} \sin \psi_j \\ -iq_j \sin \psi_j & \cos \psi_j \end{bmatrix}, \tag{1}$$

where  $\psi_j = 2\pi n_j d_j \cos(\phi_j)/\lambda$ .  $n_j$ ,  $d_j$ , and  $\phi_j$  are refractive index, thickness, and propagation angle of  $j$ th layer.  $Q_j = n_j \cos(\phi_j)$  for TE mode. As cleared in Ref (Zaky et al. 2021e), higher performance was recorded using TE polarized mode than TM mode. So, we used TE mode.  $\lambda$  is the wavelength. The characteristic matrix of the whole structure is:

$$M = \prod_j M_j = \begin{bmatrix} m_{11} & m_{12} \\ m_{21} & m_{22} \end{bmatrix} \tag{2}$$

The value of transmittance of 1D-PC multilayered structure is given as:

$$T = 100 \times \left( \frac{q_s}{q_i} \right)^2 \left| \frac{2q_i}{(m_{11} + q_s m_{12})q_i + (m_{21} + q_s m_{22})} \right|^2, \tag{3}$$

where  $q_i$  and  $q_s$  are coefficients for incident and substrate medium.

The permittivity of MCP layer can be calculated in GHz as (Awasthi et al. 2018; King et al. 2015; Nayak et al. 2017):

$$\epsilon_{plasma}(\omega) = 1 - \left[ \frac{\omega_p^2}{\omega^2 \left[ 1 - \frac{i\gamma}{\omega} \mp \frac{\omega_{gy}}{\omega} \right]} \right], \tag{4}$$

where  $\gamma$  is collision frequency and  $\omega_p$  is plasma frequency defined as  $\omega_p = \sqrt{\left( \frac{n_e e^2}{m_e \epsilon_0} \right)}$ .  $n_e$  is the number density of electron,  $\epsilon_0$  is the permittivity of vacuum ( $\epsilon_0$ ),  $m_e$  and  $e$  are the mass ( $m_e$ ) and charge ( $e$ ) of the electron, respectively. In the above equation cyclotron frequency  $\omega_{gy}$  has a dependence on magnetic field ( $B$ ) as  $\omega_{gy} = \frac{eB}{m_e}$ .

### 3 Results and discussions

Here, we consider the geometrical structure of the 1D-PC multilayered structure as clear in Fig. 1. The thicknesses of layers  $d_1$ ,  $d_2$ ,  $d_q$ ,  $d_{\text{sample}}$  are considered as 15 mm, 15 mm, 0.5 mm, 100 mm respectively. The refractive index of quartz  $n_q$  is taken as 2. The various parameters of MCP are considered as  $B$ ,  $n_e$ ,  $\gamma$ ,  $e$ ,  $m_e$  and  $\epsilon_0$  equal to 0.5 T,  $8 \times 10^{-17} \text{ m}^{-3}$ ,  $4\pi \times 10^4 \text{ Hz}$ ,  $1.6 \times 10^{-19} \text{ C}$ ,  $9.1 \times 10^{-31} \text{ kg}$  and  $8.854 \times 10^{-12} \text{ F/m}$ , respectively (King et al. 2015). The transmission is calculated using Eq. 3, and the results are plotted without and with a defect layer as shown in Fig. 2A. In this case,  $n_{\text{sample}}$  is taken as 1 (refractive index of pure air). In the case of the defect layer, a defect mode appeared in the PBG region, which has a strong dependence on the refractive index and the defect layer thickness. The transmittances at different refractive indices of the defect layer are plotted as shown in Fig. 2B. From Fig. 2B, it is seen that the resonant mode is shifted towards the lower frequency region with the increase of the dielectric constant of the sample layer.

The shift of defect mode transmittance peak with the dielectric constant of the sample layer can be used to detect the index of refraction of the sample taken as a defect. Such

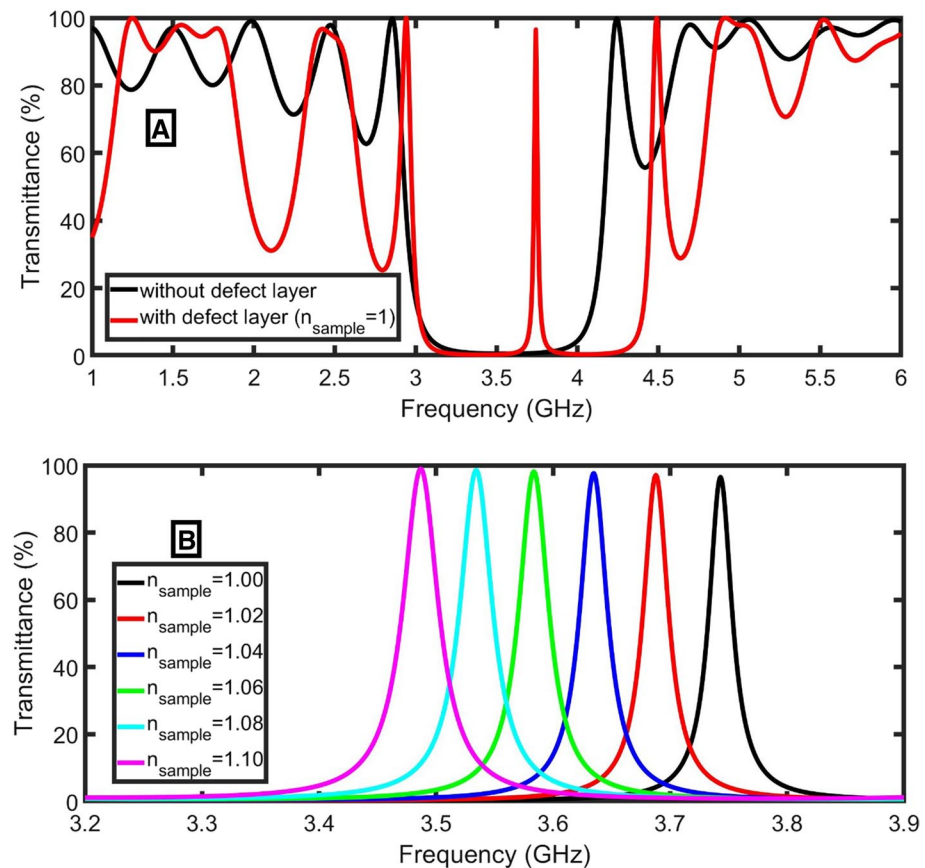


**Fig. 2** The transmittance study, **A** without and with the sample layer ( $n_{\text{sample}} = 1.00$ ), **B** for different values of  $n_{\text{sample}}$  at  $B = 0.5 \text{ T}$

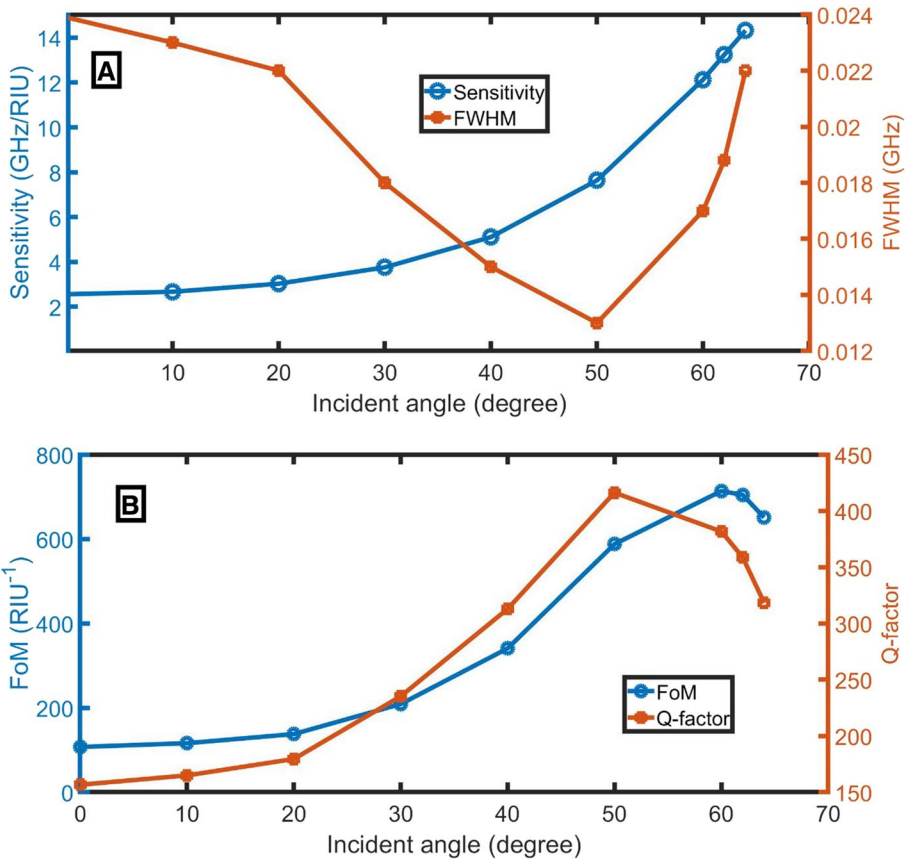


**Fig. 3** The impact of the angle of incidence on **A** sensitivity and FWHM, **B** FoM and Q-factor

properties of 1D-PC can be used as a detector. The sensitivity of the optical sensor device is measured as the fractional change of frequency ( $\Delta f_R$ ) per change in the index of refraction of the sample ( $\Delta n_s$ ). The mathematical form of sensitivity is defined as (Abadla and Elsayed 2020):

$$S = \frac{\Delta f_R}{\Delta n_s} \tag{5}$$

$$FoM = \frac{S}{FWHM} \tag{6}$$

$$Q = \frac{f_R}{FWHM} \tag{7}$$

The figure of merit (FOM) is one of the other factors to study the quality of the detector, which is the sensitivity divided by the full width at half maximum (FWHM). The quality factor is another important parameter of any sensor. It is the ratio of the central frequency ( $f_R$ ) to the FWHM. FOM provides information about the detection power of the optical

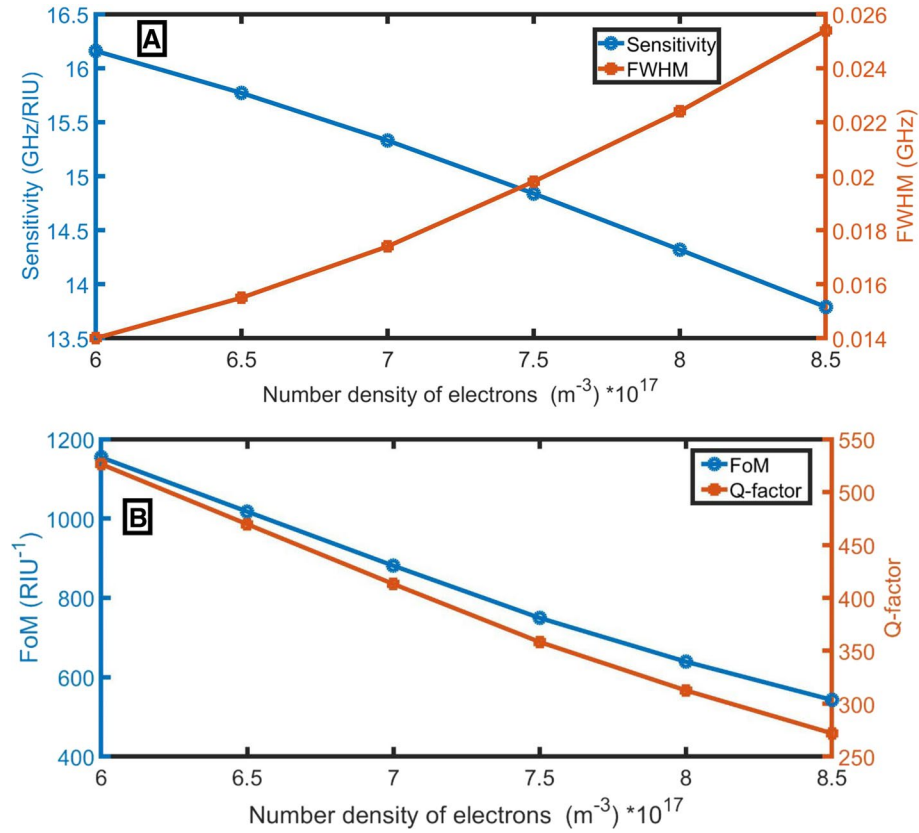


**Fig. 4** Effect of the number  $n_e$  on **A** sensitivity and FWHM, **B** FoM and Q-factor

sensor. The FWHM, sensitivity, FOM, and quality factor (Q) are calculated in the following figures.

From Fig. 3A, the sensitivity increases with the angle of incidence, whereas FWHM decreases and attain a minimum value at  $50^\circ$ , then again increases with the incident angle. Therefore, the FOM and Q-factor increase with the incident angle at lower values and attain maximum as shown in Fig. 3B. FOM is a measure of detection power of the sensor device and attains a maximum value at  $60^\circ$ . As the maximum sensitivity is at  $64^\circ$  and any further increase in the incident angle leads to the overlap between the resonant peaks, it will be used in the next study.

The sensitivity, FWHM, FoM and Q-factor are plotted with the  $n_e$  as clear in Fig. 4. From Fig. 4A, the sensitivity decreases with the increase of  $n_e$ , while the FWHM increases with  $n_e$ . Besides, both FOM and Q-factor decrease with the increase of  $n_e$  as clear in Fig. 4B. Therefore, the low value of  $n_e$  is good for the proposed sensor application as  $n_e = 6 \times 10^{17} m^{-3}$ . By decreasing  $n_e$  lower than this value, the transmittance peaks overlap.

Further, the sensitivity, FWHM, FOM and Q-factor is plotted with changing B as clear in Fig. 5. From Fig. 5A, the sensitivity increases with the increase of the B and attains saturation at 0.75 T, while the FWHM also varies with magnetic field and low value at same magnetic field 0.75 T. The FOM and Q-factor have large values at the lowest magnetic field

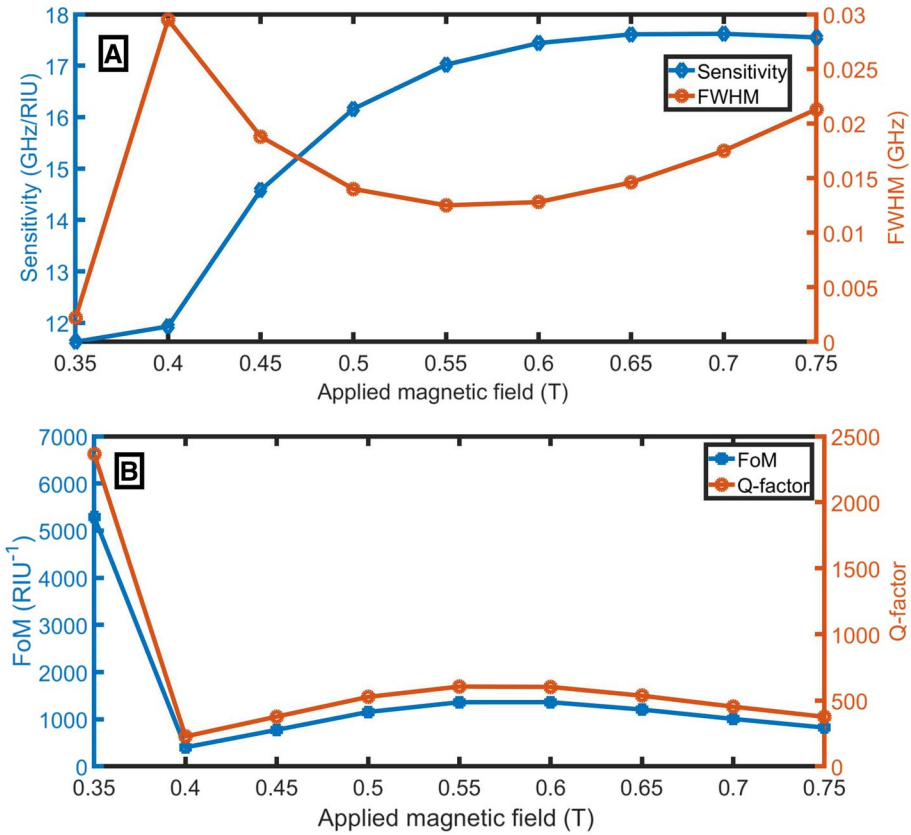


**Fig. 5** Impact of applied magnetic field on **A** sensitivity and FWHM, **B** FoM and Q-factor

but just after that the values gets decrease and attain almost saturation as shown in Fig. 5B. Therefore,  $B=0.75$  T has an optimum value, where the sensitivity and FOM have comparative large values.

Next, the sensitivity, FWHM, FoM and Q-factor are plotted with the defect layer thickness as clear in Fig. 6. From Fig. 6A, the sensitivity increases with the thickness of the defect layer and attains saturation at a higher value, whereas the FWHM shows variation with two peaks. Figure 6B shows almost a similar kind of pattern for FoM and Q-factor. Therefore, the optimum result for FoM is achieved at 60 mm and 100 mm. The sensitivity, FoM and Q-factor have the highest values at the thickness of defect layer  $d_{\text{sample}} = 100$  mm. At 100 mm there is overlap between peaks. So,  $d_{\text{sample}} = 60$  mm will be optimum.

The transmittance spectra for various samples are plotted with different optimum parameters as shown in Fig. 7. As clear in Fig. 7, the transmittance peak is shifted to the left (lower frequencies) with the increase of the sample index of refraction from 1.00 to 1.10 from 7.86 to 6.33 GHz. Besides the resonant peak shift, the PBG is red-shifted. As clear in Table 1, the proposed detector has high performance compared to other references.



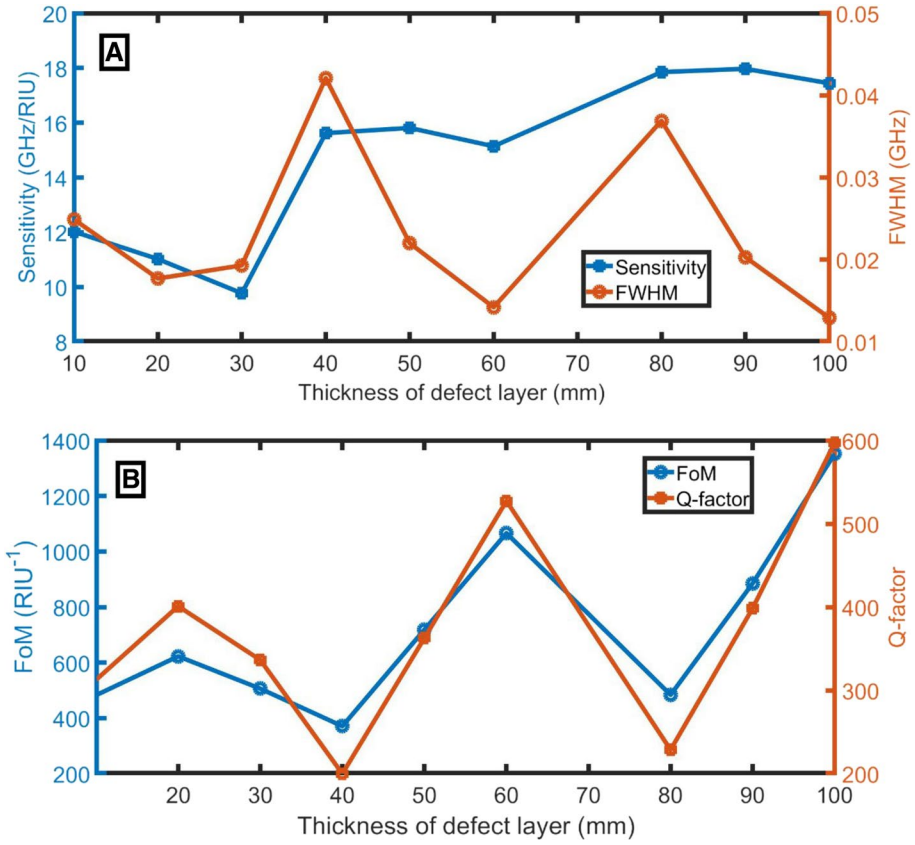


Fig. 6 Impact of the thickness of defect layer on A sensitivity and FWHM, B FoM and Q-factor

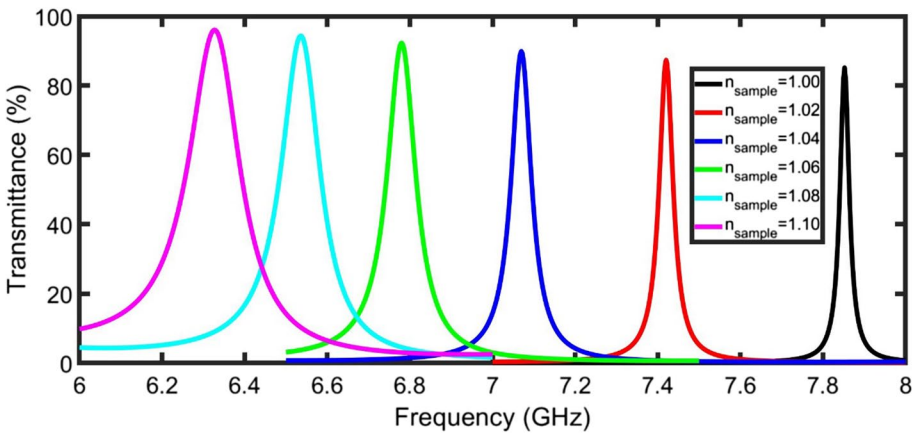


Fig. 7 The transmittance study at optimum conditions



**Table 1** Comparison study of previous study (NC = not counted)

References	S (GHz/RIU)	Q-factor	Materials
Ge and He (2014)	2.998	814	Positive and negative refractive index materials
Andueza et al. (2016)	2	NC	Matrix of photonic molecules
Panghal et al. (2019)	12.78	NC	Plasmonic hexagonal microstructured holes array in aluminum
Sun et al. (2020)	0.95	26.48	Enhanced toroidal localized spoof surface plasmons
Aly et al. (2021c)	0.496	NC	Metamaterial for measuring electric permittivity
Qin et al. (2020)	0.78	162	Toroidal metasurface
This work	15.14	527.32	1D-PC using MCP

## 4 Conclusion

In this study, a novel magnetic field-dependent detector using MCP using PC was proposed. The sensor showed a high response to the thickness of the sample layer, the applied magnetic field, the number of electron densities, and the incident angle. The optimized sensor records sensitivity of, Q- factor and FoM of 15.14 GHz/RIU, 527.32, and 1066.20 RIU<sup>-1</sup>. We are convinced that the proposed sensor is a novel optical detector and can be used in different applications.

**Acknowledgements** The authors thank the reviewers and editors for improving this article.

**Author contributions** ZAZ Invented the original idea of the study, implemented the computer code, performed the numerical simulations, analyzed the data, wrote and revised the main manuscript text. HAA Co-performed the numerical simulations. BS Co-wrote the main manuscript text and co-analyzed the data. AHA Discussed the results and supervised this work. All Authors developed the final manuscript.

**Funding** Open access funding provided by The Science, Technology &. The authors declare no fund.

**Data availability** Requests for materials or code should be addressed to Z.A.Z.

## Declarations

**Conflict of interest** The authors declare no conflict of interest.

**Human or animal rights** This article does not contain any studies involving animals or human participants performed by any of the authors.

**Open Access** This article is licensed under a Creative Commons Attribution 4.0 International License, which permits use, sharing, adaptation, distribution and reproduction in any medium or format, as long as you give appropriate credit to the original author(s) and the source, provide a link to the Creative Commons licence, and indicate if changes were made. The images or other third party material in this article are included in the article's Creative Commons licence, unless indicated otherwise in a credit line to the material. If material is not included in the article's Creative Commons licence and your intended use is not permitted by statutory regulation or exceeds the permitted use, you will need to obtain permission directly from the copyright holder. To view a copy of this licence, visit <http://creativecommons.org/licenses/by/4.0/>.

## References

- Abadla, M.M., Elsayed, H.A.: Detection and sensing of hemoglobin using one-dimensional binary photonic crystals comprising a defect layer. *Appl. Opt.* **59**, 418–424 (2020). <https://doi.org/10.1364/AO.379041>
- Abd El-Ghany, S.E.S., Noum, W.M., Matar, Z.S., Zaky, Z.A., Aly, A.H.: Optimized bio-photonic sensor using 1D-photonic crystals as a blood hemoglobin sensor. *Phys. Scr.* **96**(3), 035501 (2020). <https://doi.org/10.1088/1402-4896/abd49c>
- Afsari, A., Sarraf, M.J.: Design of a hydrogen sulfide gas sensor based on a photonic crystal cavity using graphene. *Superlattices Microstruct.* **138**, 106362 (2020). <https://doi.org/10.1016/j.spmi.2019.106362>
- Aghajamali, A.: Transmittance properties in a magnetized cold plasma–superconductor periodic multilayer. *Appl. Opt.* **55**, 6336–6340 (2016). <https://doi.org/10.1364/AO.55.006336>
- Aghajamali, A., Zare, A., Wu, C.-J.: Analysis of defect mode in a one-dimensional symmetric double-negative photonic crystal containing magnetized cold plasma defect. *Appl. Opt.* **54**, 8602–8606 (2015). <https://doi.org/10.1364/AO.54.008602>
- Akahane, Y., Asano, T., Song, B.-S., Noda, S.: High-Q photonic nanocavity in a two-dimensional photonic crystal. *Nature* **425**, 944–947 (2003). <https://doi.org/10.1038/nature02063>
- Aly, A.H., Zaky, Z.A.: Ultra-sensitive photonic crystal cancer cells sensor with a high-quality factor. *Cryogenics* **104**, 102991 (2019). <https://doi.org/10.1016/j.cryogenics.2019.102991>
- Aly, A.H., Zaky, Z.A., Shalaby, A.S., Ahmed, A.M., Vigneswaran, D.: Theoretical study of hybrid multifunctional one-dimensional photonic crystal as a flexible blood sugar sensor. *Phys. Scr.* **95**, 035510 (2020). <https://doi.org/10.1088/1402-4896/ab53f5>
- Aly, A.H., Awasthi, S., Mohamed, A., Matar, Z., Mohaseb, M., Al-Dossari, M., et al.: Detection of reproductive hormones in females by using 1D photonic crystal-based simple reconfigurable biosensing design. *Crystals* **11**, 1533 (2021a). <https://doi.org/10.3390/cryst11121533>
- Aly, A.H., Mohamed, D., Zaky, Z.A., Matar, Z.S., Abd El-Gawaad, N.S., Shalaby, A.S., Tayeboun, F., Mohaseb, M.: Novel biosensor detection of tuberculosis based on photonic band gap materials. *Mater. Res.* (2021). <https://doi.org/10.1590/1980-5373-mr-2020-0483>
- Aly, A.H., Ameen, A.A., Mahmoud, M.A., Matar, Z.S., Al-Dossari, M., Elsayed, H.A.: Photonic crystal enhanced by metamaterial for measuring electric permittivity in GHz range. *Photonics* **8**, 416 (2021c). <https://doi.org/10.3390/photonics8100416>
- Andueza, A., Pérez-Conde, J., Sevilla, J.: Differential refractive index sensor based on photonic molecules and defect cavities. *Opt. Express* **24**, 18807–18816 (2016). <https://doi.org/10.1364/OE.24.018807>
- Armstrong, E., O'Dwyer, C.: Artificial opal photonic crystals and inverse opal structures: fundamentals and applications from optics to energy storage. *J. Mater. Chem. C* **3**, 6109–6143 (2015). <https://doi.org/10.1039/C5TC01083G>
- Askari, N., Mirzaie, R., Eslami, E.: Analysis of band structure, transmission properties, and dispersion behavior of THz wave in one-dimensional parabolic plasma photonic crystal. *Phys. Plasmas* **22**, 112117 (2015)
- Augu  , B., Fuertes, M.C., Angelom  , P.C., Abdala, N.L., Soler, G.J.A.A., Illia, A.F.: Tamm plasmon resonance in mesoporous multilayers: toward a sensing application. *ACS Photonics* **1**(9), 775–780 (2014). <https://doi.org/10.1021/ph5001549>
- Awasthi, S.K., Panda, R., Shiveshwari, L.: Multichannel tunable filter properties of 1D magnetized ternary plasma photonic crystal in the presence of evanescent wave. *Phys. Plasmas* **24**, 072111 (2017). <https://doi.org/10.1063/1.4989703>
- Awasthi, S.K., Panda, R., Chauhan, P.K., Shiveshwari, L.: Multichannel tunable omnidirectional photonic band gaps of 1D ternary photonic crystal containing magnetized cold plasma. *Phys. Plasmas* **25**, 052103 (2018). <https://doi.org/10.1063/1.5026547>
- Ayyub, O.B., Ibrahim, M.B., Briber, R.M., Kofinas, P.: Self-assembled block copolymer photonic crystal for selective fructose detection. *Biosens. Bioelectron.* **46**, 124–129 (2013). <https://doi.org/10.1016/j.bios.2013.02.025>
- Bikbaev, R.G., Vetrov, S.Y., Timofeev, I.V.: Optical Tamm states at the interface between a photonic crystal and a gyroid layer. *J. Opt. Soc. Am. B* **34**, 2198–2202 (2017). <https://doi.org/10.1364/JOSAB.34.002198>
- Boopathi, C., Kumar, K.V., Sheebarani, S., Selvakumar, K., Rashed, A.N.Z., Yupapin, P.: Design of human blood sensor using symmetric dual core photonic crystal fiber. *Results Phys.* **11**, 964–965 (2018). <https://doi.org/10.1016/j.rinp.2018.10.065>
- Buswell, S., Wright, V., Buriak, J., Van, V., Evoy, S.: Specific detection of proteins using photonic crystal waveguides. *Opt. Express* **16**, 15949–15957 (2008). <https://doi.org/10.1364/OE.16.015949>

- Chang, T.-W., Chien, J.-R.C., Wu, C.-J.: Magnetic-field tunable multichannel filter in a plasma photonic crystal at microwave frequencies. *Appl. Opt.* **55**, 943–946 (2016). <https://doi.org/10.1364/AO.55.000943>
- Dehnavi, Z.N., Askari, H.R., Malekshahi, M., Dorrani, D.: Investigation of tunable omnidirectional band gap in 1D magnetized full plasma photonic crystals. *Phys. Plasmas* **24**(9), 093517 (2017). <https://doi.org/10.1063/1.5004695>
- El Beheiry, M., Liu, V., Fan, S., Levi, O.: Sensitivity enhancement in photonic crystal slab biosensors. *Opt. Express* **18**, 22702–22714 (2010). <https://doi.org/10.1364/OE.18.022702>
- Gao, W., Hu, X., Li, C., Yang, J., Chai, Z., Xie, J., et al.: Fano-resonance in one-dimensional topological photonic crystal heterostructure. *Opt. Express* **26**, 8634–8644 (2018). <https://doi.org/10.1364/OE.26.008634>
- Ge, X., He, S.: Experimental realization of an open cavity. *Sci. Rep.* **4**, 1–5 (2014). <https://doi.org/10.1038/srep05965>
- Hidalgo, N., Calvo, M.E., Colodrero, S., Miguez, H.: Porous one-dimensional photonic crystal coatings for gas detection. *IEEE Sens. J.* **10**, 1206–1212 (2010). <https://doi.org/10.1109/JSEN.2010.2043525>
- Inoue, M., Fujikawa, R., Baryshev, A., Khanikaev, A., Lim, P., Uchida, H., et al.: Magnetophotonic crystals. *J. Phys. D Appl. Phys.* **39**, R151–R161 (2006)
- John, S.: Strong localization of photons in certain disordered dielectric superlattices. *Phys. Rev. Lett.* **58**, 2486–2489 (1987). <https://doi.org/10.1103/PhysRevLett.58.2486>
- John, S., Florescu, M.: Photonic bandgap materials: towards an all-optical micro-transistor. *J. Opt. A Pure Appl. Opt.* **3**, S103–S120 (2001). <https://doi.org/10.1088/1464-4258/3/6/361>
- Kamboj, G., Yadav, R., Kaler, R.: A single column plasma photonic crystal (SC-PPC). *Phys. Plasmas* **28**, 053509 (2021)
- Kim, S., Lee, J., Jeon, H., Kim, H.J.: Fiber-coupled surface-emitting photonic crystal band edge laser for biochemical sensor applications. *Appl. Phys. Lett.* **94**, 133503 (2009). <https://doi.org/10.1063/1.3114405>
- King, T.-C., Yang, C.-C., Hsieh, P.-H., Chang, T.-W., Wu, C.-J.: Analysis of tunable photonic band structure in an extrinsic plasma photonic crystal. *Phys. E Low Syst. Nanostruct.* **67**, 7–11 (2015). <https://doi.org/10.1016/j.physe.2014.11.001>
- Kumar, A., Kumar, N., Thapa, K.B.: Tunable broadband reflector and narrowband filter of a dielectric and magnetized cold plasma photonic crystal. *Eur. Phys. J. Plus* **133**, 1–8 (2018). <https://doi.org/10.1140/epjp/i2018-12073-3>
- Kushwaha, A.S., Kumar, A., Rajeev Kumar, S.K.: A study of surface plasmon resonance (SPR) based biosensor with improved sensitivity. *Photonics Nanostruct. Fundam. Appl.* **31**, 99–106 (2018). <https://doi.org/10.1016/j.photonics.2018.06.003>
- Liu, W., Wu, J.-W.: Tunable optical bistability at microwave frequency based on 1D sandwich photonic structure consisting of a nonlinear dielectric slab and two magnetized cold plasma layers. *Curr. Appl. Phys.* **29**, 66–71 (2021)
- Lyubchanskii, I., Dadoenkova, N., Lyubchanskii, M., Shapovalov, E., Rasing, T.: Magnetic photonic crystals. *J. Phys. D Appl. Phys.* **36**, R277–R287 (2003)
- Meradi, K.A., Tayeboun, F., Guerinik, A., Zaky, Z.A., Aly, A.H.: Optical biosensor based on enhanced surface plasmon resonance: theoretical optimization. *Opt. Quant. Electron.* **54**, 1–11 (2022). <https://doi.org/10.1007/s11082-021-03504-8>
- Nayak, C., Aghajamali, A., Saha, A.: Double-negative multilayer containing an extrinsic random layer thickness magnetized cold plasma photonic quantum-well defect. *Superlattices Microstruct.* **111**, 248–254 (2017). <https://doi.org/10.1016/j.spmi.2017.06.041>
- Nobahar, D., Hajisharifi, K., Mehdian, H.: Twisted beam shaping by plasma photonic crystal. *J. Appl. Phys.* **124**, 213102 (2018)
- Panda, A., Devi, P.P.: Photonic crystal biosensor for refractive index based cancerous cell detection. *Opt. Fiber Technol.* **54**, 102123 (2020). <https://doi.org/10.1016/j.yofte.2019.102123>
- Panda, A., Pukhrambam, P.D., Wu, F., Belhadj, W.: Graphene-based 1D defective photonic crystal biosensor for real-time detection of cancer cells. *Eur. Phys. J. Plus* **136**, 1–19 (2021). <https://doi.org/10.1140/epjp/s13360-021-01796-z>
- Pandey, A., Tripathi, A., Srivastava, S., Jit, S.: Analysis of ternary layer photonic band gap tunable filters for wavelength division multiplexing applications. *J. Nanoelectron. Optoelectron.* **12**, 331–336 (2017). <https://doi.org/10.1166/jno.2017.2021>
- Panghal, A., Jain, R. K., Pattanayak, A., Bhattacharya, A., Achanta, V. G. Prabhu S. : Terahertz chemical sensor based on the plasmonic hexagonal microstructured holes array in aluminum. In: 2019 44th international conference on infrared, millimeter, and terahertz waves (IRMMW-THz). 1–2 (2019)

- Qin, P., Li, E., Li, T., Ma, H., Yang, Y., Ang, L.K., et al.: Angle-insensitive toroidal metasurface for high-efficiency sensing. *IEEE Trans. Microw. Theory Tech.* **69**, 1511–1517 (2020). <https://doi.org/10.1109/TMTT.2020.3027016>
- Rajasekar, R., Robinson, S.: Nano-pressure and temperature sensor based on hexagonal photonic crystal ring resonator. *Plasmonics* **14**, 3–15 (2019). <https://doi.org/10.1007/s11468-018-0771-x>
- Sakai, O., Sakaguchi, T., Tachibana, K.: Photonic bands in two-dimensional microplasma arrays I: theoretical derivation of band structures of electromagnetic waves. *J. Appl. Phys.* **101**, 073304 (2007)
- Shiri, R., Khalkhali, T.F., Shahrokhbadi, H., Bananej, A.: Designing one-dimensional magnetized plasma photonic crystals for compensating second-and third-order dispersion effects in ultra-short pulse lasers. *Optik* **188**, 137–146 (2019)
- Sun, B., Yu, Y., Yang, W.: Enhanced toroidal localized spoof surface plasmons in homolateral double-split ring resonators. *Opt. Express* **28**, 16605–16615 (2020). <https://doi.org/10.1364/OE.395068>
- Tammam, M.T., Zaky, Z.A., Arvind Sharma, Z.S., Matar, A.H., Aly, M.A.M.: Defected photonic crystal array using porous GaN as malaria sensor. *IOP Conf. Series Mater. Sci. Eng.* **1171**(1), 012005 (2021). <https://doi.org/10.1088/1757-899X/1171/1/012005>
- Tandaechanurat, A., Ishida, S., Guimard, D., Nomura, M., Iwamoto, S., Arakawa, Y.: Lasing oscillation in a three-dimensional photonic crystal nanocavity with a complete bandgap. *Nat. Photonics* **5**, 91–94 (2011). <https://doi.org/10.1038/nphoton.2010.286>
- Wang, Y., Liu, S., Zhong, S.: Tunable multichannel terahertz filtering properties of dielectric defect layer in one-dimensional magnetized plasma photonic crystal. *Opt. Commun.* **473**, 125985 (2020). <https://doi.org/10.1016/j.optcom.2020.125985>
- Yablonovitch, E.: Photonic crystals: semiconductors of light. *Sci. Am.* **285**, 46–55 (2001). <https://doi.org/10.1038/scientificamerican1201-46>
- Yablonovitch, E., Gmitter, T.: Photonic band structure: the face-centered-cubic case. *Phys. Rev. Lett.* **63**, 1950–1953 (1989). <https://doi.org/10.1103/PhysRevLett.63.1950>
- Zakhidov, A.A., Baughman, R.H., Iqbal, Z., Cui, C., Khayrullin, I., Dantas, S.O., et al.: Carbon structures with three-dimensional periodicity at optical wavelengths. *Science* **282**, 897–901 (1998). <https://doi.org/10.1126/science.282.5390.897>
- Zaky, Z.A., Aly, A.H.: Theoretical study of a tunable low-temperature photonic crystal sensor using dielectric-superconductor nanocomposite layers. *J. Supercond. Novel Magn.* **33**, 2983–2990 (2020). <https://doi.org/10.1007/s10948-020-05584-1>
- Zaky, Z.A., Aly, A.H.: Modeling of a biosensor using Tamm resonance excited by graphene. *Appl. Opt.* **60**, 1411–1419 (2021a). <https://doi.org/10.1364/AO.412896>
- Zaky, Z.A., Aly, A.H.: Highly sensitive salinity and temperature sensor using Tamm resonance. *Plasmonics* **16**, 2315–2325 (2021b). <https://doi.org/10.1007/s11468-021-01487-6>
- Zaky, Z.A., Aly, A.H.: Gyroidal graphene/porous silicon array for exciting optical Tamm state as optical sensor. *Sci. Rep.* **11**, 19389 (2021c). <https://doi.org/10.1038/s41598-021-98305-0>
- Zaky, Z.A., Ahmed, A.M., Shalaby, A.S., Aly, A.H.: Refractive index gas sensor based on the Tamm state in a one-dimensional photonic crystal: theoretical optimisation. *Sci. Rep.* **10**, 9736 (2020). <https://doi.org/10.1038/s41598-020-66427-6>
- Zaky, Z.A., Aly, A.H., Moustafa, B.: Plasma cell sensor using photonic crystal cavity. *Opt. Quant. Electron.* **53**, 591 (2021a). <https://doi.org/10.1007/s11082-021-03201-6>
- Zaky, Z.A., Ahmed, Ashour M., Aly, Arafah H.: Remote temperature sensor based on Tamm resonance. *Silicon* (2021). <https://doi.org/10.1007/s12633-021-01064-w>
- Zaky, Z.A., Sharma, A., Aly, A.H.: Gyroidal graphene for exciting Tamm plasmon polariton as refractive index sensor: theoretical study. *Opt. Mater.* **122**, 111684 (2021c). <https://doi.org/10.1016/j.optmat.2021.111684>
- Zaky, Z.A., Sharma, A., Aly, A.H.: Tamm plasmon polariton as refractive index sensor excited by gyroid metals/porous Ta<sub>2</sub>O<sub>5</sub> photonic crystal. *Plasmonics* (2021). <https://doi.org/10.1007/s11468-021-01559-7>
- Zaky, Z.A., Sharma, A., Alamri, S., Saleh, N., Aly, A.H.: Detection of fat concentration in milk using ternary photonic crystal. *Silicon* (2021). <https://doi.org/10.1007/s12633-021-01379-8>
- Zaky, Z.A., Sharma, A., Alamri, S., Aly, A.H.: Theoretical evaluation of the refractive index sensing capability using the coupling of Tamm-Fano resonance in one-dimensional photonic crystals. *Appl. Nanosci.* **11**, 2261–2270 (2021f). <https://doi.org/10.1007/s13204-021-01965-7>
- Zegadi, R., Ziet, L., Zegadi, A.: Design of high sensitive temperature sensor based on two-dimensional photonic crystal. *Silicon* **12**, 2133–2139 (2019). <https://doi.org/10.1007/s12633-019-00303-5>
- Zhang, H.-F., Liu, S.-B., Kong, X.-K.: Photonic band gaps in one-dimensional magnetized plasma photonic crystals with arbitrary magnetic declination. *Phys. Plasmas* **19**, 122103 (2012). <https://doi.org/10.1063/1.4766474>

Zhou, Z., Wan, B., Xu, Y., Ma, Y., Zhang, H., Zhang, D.: Tunable zero-phase delay of one-dimensional photonic crystals containing InSb material. *J. Opt. Soc. Am. B* **38**, 114–122 (2021). <https://doi.org/10.1364/JOSAB.404852>

**Publisher's Note** Springer Nature remains neutral with regard to jurisdictional claims in published maps and institutional affiliations.